Role of Parallel Flow in the Improved Mode on the STOR-M Tokamak

S. Sen,[1,*] C. Xiao,[2] A. Hirose,[2] and R. A. Cairns[3]
[1]*Kyoto University, Kyoto, Japan*
[2]*University of Saskatchewan, Saskatoon, Canada*
[3]*University of St. Andrews, St. Andrews, United Kingdom*
(Received 26 October 1999; published 17 April 2002)

A novel feature of the H-mode induced by compact torus injection on the STOR-M tokamak is observed. There is almost no change in the radial electric field profiles during and after the L-H transition. The usual hypothesis of the $\mathbf{E} \times \mathbf{B}$ shear stabilization mechanism is therefore unlikely to play a role in this transition. A new mechanism of the stabilization of microinstabilities by parallel flow is suggested as the plausible cause for the transition to this improved regime.

DOI: 10.1103/PhysRevLett.88.185001 PACS numbers: 52.55.Hc, 52.55.Fa

I. Introduction.—An important challenge for enhanced tokamak operation is the development and understanding of the basic physics involved in the process that leads to the transition to the improved confinement modes. A popular picture of the H-mode has rapidly grown up: Some mechanism(s) (ion orbit loss, poloidal asymmetry in the transport, and/or Reynolds stress) creates an equilibrium radial electric field which gives rise to a *perpendicular* $\mathbf{E} \times \mathbf{B}$ drift, which in turn stabilizes microinstabilities and, as a result, fluctuation is suppressed and confinement is improved—the so-called H-mode. Similarly, the transition to the VH-mode is also attributed to the $\mathbf{E} \times \mathbf{B}$ shear, here the shear is provided by the shear in the toroidal flow. Most recently, the $\mathbf{E} \times \mathbf{B}$ shear stabilization mechanism has also been proposed to explain the core transport barrier formation during the NCS or ERS modes. It is believed that the change in the radial electric field in the core is produced in a number of ways, for example, by toroidal flow and/or by pressure gradient and, more recently, by poloidal flow. Parallel flow (and/or its shear), on the other hand, is in general not considered to be related to the improved regimes of confinement.

In the recently found H-mode induced by compact torus (CT) injection on the Saskatchewan Torus-Modified (STOR-M) tokamak, all the signatures of H-modes, such as an increase in the electron density, significant reduction in the H_α radiation level, steepening of the edge density profile, and suppression of floating potential fluctuations, are observed [1]. However, one of the distinctive features on the STOR-M is that there is almost no change in the radial electric field profiles during and after the L-H transition. Consequently, the usual hypothesis of the $\mathbf{E} \times \mathbf{B}$ shear stabilization mechanism is unlikely to play a role in the transition.

In this Letter, we report this novel feature of the CT induced H-modes on the STOR-M and suggest a new mechanism for the improvement in the confinement. We propose that the tangential CT injection can introduce a considerable amount of momentum input which can generate toroidal flows. We demonstrate that the flow curvature in the parallel flow (note the parallel flow in the tokamak is almost equal to the toroidal flow) stabilizes resistive drift-ballooning modes, which have been identified as the likely mechanism for anomalous transport in the plasma [2,3]. We also demonstrate that the scale length of the flow profile necessary for this stabilization is rather modest. As no *perpendicular* component of flow and/or its shear is involved in the mechanism, no change in the radial electric field is therefore expected. This, thus, explains the improvement in the confinement observed on the STOR-M which does not usually observe any change in the radial electric field during and after the transition.

II. Experimental results.—The experiment was carried out on the STOR-M tokamak with University of Saskatchewan Compact Torus Injection (USCTI). Hydrogen was used for both CT and tokamak discharges. USCTI has a coaxial configuration with formation, compression, and acceleration sections. The inner and outer diameters of the acceleration sections are 10 and 3.6 cm, respectively. The typical CT parameters at the exit of the CT injector are 15 cm in length, $(1-2) \times 10^{15}$ cm^{-3} in density, and 120–200 km/s in velocity. The CT mass is 1 μg, and its particle inventory is approximately 50% of that in the STOR-M tokamak. The CT was injected at an angle of 27° with respect to the horizontal normal of the tokamak. The major and minor radii of the STOR-M tokamak are 45 and 12 cm, respectively. The arrangement of the limiter in the STOR-M allows a plasma horizontal displacement up to 1 cm without being scraped off. A rake Langmuir probe array was also installed to measure plasma parameters at the tokamak edge. The nominal plasma parameters were $B_t = 0.8$ T, $I_p = 20$ kA, and $n_e = (0.5-2) \times 10^{13}$ cm^{-3}. More details about the experiment can be found in Ref. [1].

Figure 1 shows the waveforms of the tokamak discharge parameters with a CT injected at $t = 15$ ms. The traces shown are (from top) plasma current (I_p), loop voltage (V_l), electron density ($\bar{n}_e$), horizontal displacement (Δ_H), H_α radiation intensity, and estimated global energy confinement time (τ_E). Following the CT injection, the discharge current and loop voltage remain almost intact, indicating a constant Spitzer temperature. The electron

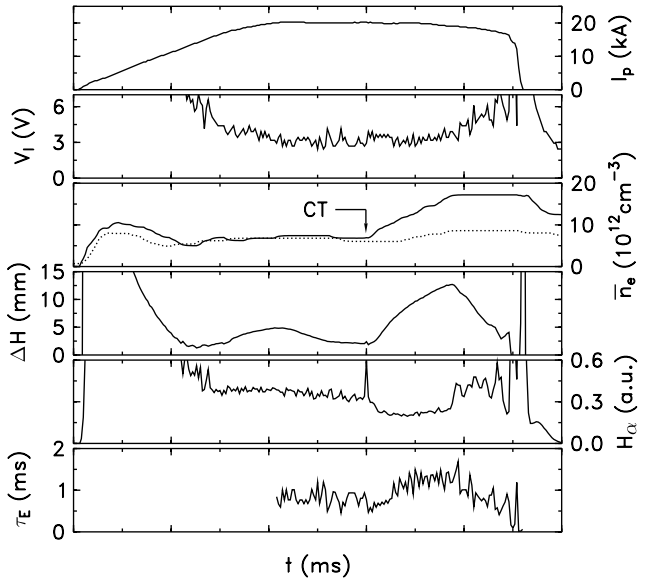

FIG. 1. Time history of tokamak discharge parameters (shot No. 120558): discharge current, loop voltage, line averaged electron density, horizontal displacement, H_α radiation level, and global energy confinement time.

density increases more than twofold from 0.75×10^{13} to 1.7×10^{13} cm^{-3} at a rate of approximately 1.9×10^{15} cm$^{-3} \cdot$ s^{-1}. This high density phase remains until the end of the discharge. The plasma position shifts outwards during the high confinement phase $15 < t < 19.5$ ms. The H_α radiation level decreases abruptly by approximately 35% following the CT injection and returns to the normal level at $t = 19.5$ ms, indicating an L-H transition and an H-L back transition, respectively. During the H-mode phase (from 15 to 19.5 ms) the global energy confinement time increases from 0.9 ms (prior to CT injection) to 1.4 ms. Since the electron temperature did not change significantly, the global energy confinement improvement was mainly due to improved particle confinement. The potential fluctuations were measured with a Langmuir probe array extending from the scrape-off layer to the tokamak edge region. In both regions, the density fluctuation levels decrease significantly after CT injection. The reduction in potential fluctuations coincides with the H-mode phase. The Langmuir probe array was also used to measure electron density and floating potential profiles. Figure 2 depicts the waveform of the electron density with a CT injected at $t = 15.5$ ms. The local density decreases for about 1 ms after CT injection, in contrast to a prompt increase in the line averaged density. This suggests a sudden reduction in the outwards particle flow due to formation of a transport barrier in the region $r < 10.9$ cm, which is not accessible with the Langmuir probe array. Figure 3 shows that the density profile becomes more steepened in the improved confinement phase and relaxes to the preinjection profile after H-L transition. The floating potential during the improved confinement phase increases as shown in Fig. 4. Following CT injection, the floating potential

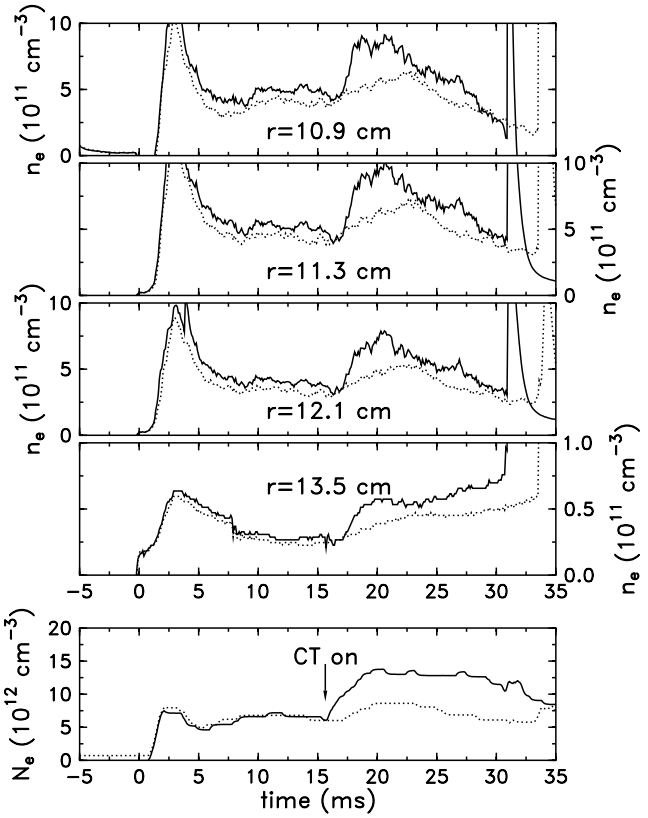

FIG. 2. Waveforms of electron density at the tokamak edge with CT injection (solid lines, shot No. 121194). The dotted lines represent the electron density for the case without CT discharge, but with gas injection into the CT injector. The last frame depicts the line averaged electron density.

increases instantly in all locations accessible with probes. However, the remarkable feature is that there is almost no change in the radial electric field. There is a little change in the temperature during the transition. Hence, the contribution coming from the sheath potential to E_r is

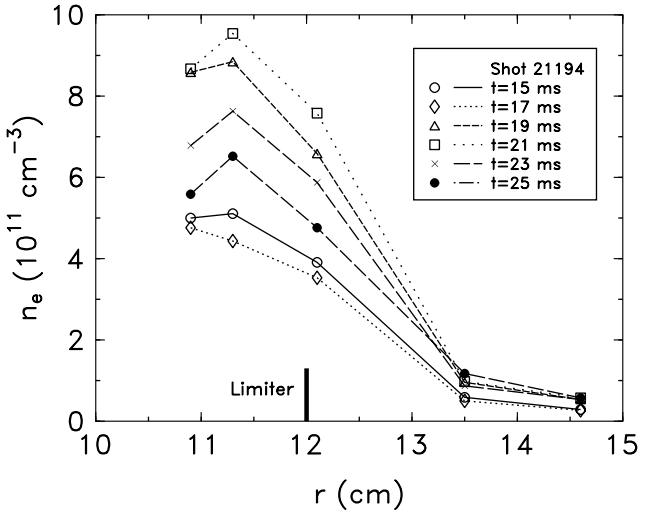

FIG. 3. Electron density profiles at the tokamak edge with CT injection (solid lines, shot No. 121194).

less (as it is the change in the potential which contributes to E_r). So, there is *even less* contribution from the sheath potential to the E_r shear (as it is the second radial derivative of the potential). The electron temperature is measured by quickly scanning the bias voltage of a single probe as described in detail in our earlier work [2], where a significant power was injected (180 kW) with a preferential skin heating at the edge; whereas, in the case of CT injection, the power injection associated with the CT is small resulting in very little change in the temperature.

III. Theoretical results.—With these experimental observations in mind, we now develop the theory of dissipative (resistive) drift-ballooning modes in the presence of parallel flow. The dissipative drift-ballooning modes have recently been identified as the likely mechanism for anomalous transport in the plasma edge [3,4] and also appear to be the most appropriate candidate to get stabilized in the improved mode on the STOR-M, because the experiments observe a sharp increase in the electron density in the edge of the STOR-M (Figs. 2 and 3), whereas the temperature does not change significantly (so temperature gradient driven instabilities are not likely to play a major role here). We use the usual (r, θ, ξ) coordinates, corresponding to the minor radial, poloidal, and toroidal directions, respectively, and consider the long-wavelength ($k_\theta^2 \rho_s^2 \ll 1$) drift waves for a large aspect-ratio circular tokamak. The perturbed potential can then be expressed as

$$\phi(\vec{x}, t) \equiv \phi(\rho, \theta, \xi, t) = \phi(\rho, \theta) \exp[i(n\xi - m_0\theta - \omega t)],$$

where $\rho = (r - r_0)$, r_0 is the radius of the reference mode rational surface, i.e., $m_0 = nq(r_0)$, $k_\theta = \frac{m_0}{r_0}$, and $\hat{s} = \frac{rq'}{q}$ at $r = r_0$. Here, for simplicity, we will assume the ions to be cold and will ignore the electron temperature gradient. Using fluid descriptions, the eigenvalue equation in the presence of a velocity field can be derived in a straightforward way [5–7]:

$$\left[(1 - i\delta)(\omega - k_\parallel V_{\parallel o})\rho_s^2\left(\frac{\partial^2}{\partial \rho^2} - k_\theta^2\right) + (\omega_e^* - \omega + k_\parallel V_{\parallel o}) - \frac{\omega_e^{*2}}{(\omega - k_\parallel V_{\parallel o})}\left(\frac{\epsilon_c}{k_\theta \rho_s}\right)^2\left(\frac{\partial}{\partial \theta} + ik_\theta \rho \hat{s}\right)^2 - 2(1 - i\delta)\epsilon_n \omega_e^*\left(\cos\theta + \frac{i \sin\theta}{k_\theta}\frac{\partial}{\partial \rho}\right) - \frac{dV_{\parallel o}}{d\rho}\frac{k_\theta \rho_s k_\parallel C_s}{(\omega - k_\parallel V_{\parallel o})} - \frac{\rho^2 \omega_e^*}{L_*^2}\right]\phi = 0, \quad (1)$$

where $\rho_s^2 = (C_S^2/\omega_{ci}^2)$, $C_S^2 = \frac{T_e}{m_i}$, $\epsilon_n = q\epsilon_c = L_n/R$, $\delta = \nu_{ei} m_e \omega / k_\parallel^2 T_e$, $V_{\parallel o}(\rho)$ is the equilibrium parallel velocity, $\omega_e^*(\rho)$ is the diamagnetic drift frequency, and L_* is the density gradient variation scale length and typically of the order of density scale length L_n. We remind the readers that our "δ" should not be confused with that in the standard "$i\delta$" model representing the nonadiabatic electron response. The first term in Eq. (1) arises from the finite Larmour radius effect and the third from the ion sound. The fourth is the effect of toroidal coupling, whereas the last term introduces the radial variation of ω_e^* with $L_*^{-2} = (1/\omega_e^*)[(d^2\omega_e^*/d\rho^2)]$.

Now to model the equilibrium parallel velocity we follow the toroidal velocity profile usually observed on the STOR-M during the positive bias phase [8] (note, this is, however, a general profile obtained by the usual Taylor expansion):

$$V_{\parallel o}(\rho) \equiv V_{\parallel oo} - \left(\frac{\rho}{L_{v1}} + \frac{\rho^2}{L_{v2}^2}\right)V_{\parallel oo},$$

where

$$\frac{dV_{\parallel o}}{d\rho} = \frac{V_{\parallel oo}}{L_{v1}}, \qquad \frac{1}{2}\frac{d^2 V_{\parallel o}}{d\rho^2} = \frac{V_{\parallel oo}}{L_{v2}^2}.$$

To reduce the two-dimensional (2D) eigenmode problem to one-dimensional (1D), we will apply the ballooning transformation. As as been mentioned elsewhere [9], the usual restriction on the applicability of the conventional ballooning formalism in the presence of flow shear does not apply for pure *parallel* flows. In the usual theory of high n ballooning modes [10], one maps the poloidal angle θ onded coordinate χ with $-\infty < \chi < \infty$ and writes the perturbation in the form

$$\phi(\theta, x) = \sum_m e^{-im\theta} \int_{-\infty}^{\infty} e^{im\chi} \hat{\phi}(\chi, x)\, d\chi,$$
$$\text{where } \hat{\phi} = A(x)F(\chi, x) \exp[-ix(\chi + \chi_0)],$$

where χ_0 is an arbitrary phase of the eikonal and $x = k_\theta \rho \hat{s}$. Here, $A(x)$ is assumed to vary on some scale intermediate between the equilibrium scale length and the perpendicular wavelength. Now to leading order (in $n^{-1/2}$ expansion) the ballooning equation becomes

$$\left[\frac{\omega_e^{*2}}{\omega^2}\left(\frac{\epsilon_c}{k_\theta \rho_s}\right)^2 \frac{\partial^2}{\partial \chi^2} - (\omega_e^* - \omega)/\omega + 2(1 - i\delta)\epsilon_n \frac{\omega_e^*}{\omega}[\cos\chi + \hat{s}(\chi + \chi_o)\sin\chi] - \frac{1}{4}\left(\frac{dV_{\parallel o}}{d\rho}\frac{k_\theta \rho_s C_s}{\omega^2 qR}\right)^2 \Big/ \frac{\omega_e^{*2}}{\omega^2}\left(\frac{\epsilon_c}{k_\theta \rho_s}\right)^2 + (k_\theta \rho)^2(1 - i\delta)[1 + \hat{s}^2(\chi + \chi_o)^2] + \frac{\rho^2 \omega_e^*}{L_*^2 \omega}\right]\xi = 0. \quad (2)$$

In deriving Eq. (2), the first derivative (with respect to χ) term has been removed by suitably changing the dependent variable (to ξ). We have not preassigned any ordering for δ, although for the context of the present work δ will be assumed to be $\ll 1$, which, in fact, is the regime most relevant to the edge plasma. Restricting ourselves to this

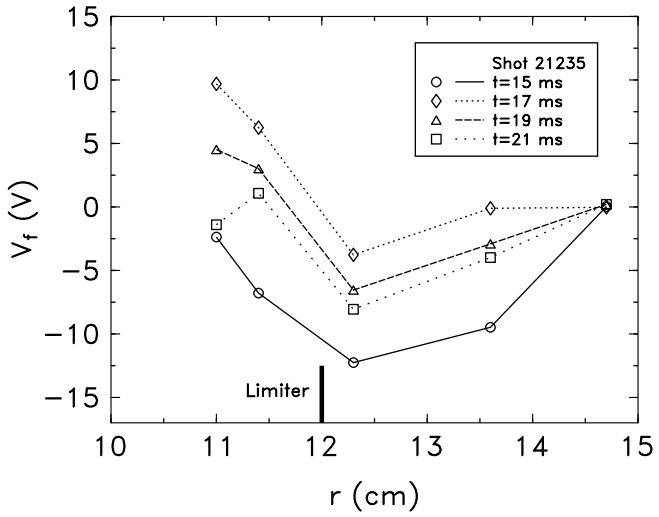

FIG. 4. Floating potential profiles in the tokamak edge region with CT injection (solid lines, shot No. 121235).

limit ($\delta \ll 1$), however, considerably simplifies the subsequent mathematical analysis. Any x variation arising due to δ then becomes insignificant, and one can then treat δ as a constant.Assuming δ constant then reduces the otherwise fourth-order differential eigenmode equation to one second-order ordinary differential Eq. (2).

Now to explore the implication of the velocity profile on the radial structure and on the stability of the modes, one needs the higher-order ballooning theory. We notice that the second-order differential operator defined by Eq. (2) is "self-adjoint" (even though it is complex) for functions $\xi(\chi, \rho)$ which $\rightarrow 0$ as $\chi \rightarrow \infty$. This allows us to use the higher-order ballooning theory of Hastie *et al.* [10] originally developed for collisionless drift waves. In the higher-order theory, χ_o is obtained from the equation $\frac{\partial \Omega}{\partial \chi_o}(x, \chi_0) = 0$ and the radial envelope function $A(x)$ satisfies

$$\frac{\partial^2 \Omega}{\partial \chi_0^2}\frac{d^2A}{dx^2} + [2(\Omega - \Omega_0) - p_1 - 2p_2 x^2]A = 0, \tag{3}$$

where, $\Omega = [1/k_\theta^2 \rho_s^2 \hat{s}^2)][\frac{\omega_e^*}{\omega} - 1 - (1 - i\delta)k_\theta^2 \rho_s^2]$, $\Omega_0 = i[\epsilon_c/(k_\theta^2 \rho_s^2 \hat{s})]$, $p_1 = \frac{1}{2}(\frac{C_s V_{\|o}}{\omega^2 qR\hat{s}L_{v1}})^2/(\omega_e^{*2}/\omega^2)(\frac{\epsilon_c}{k_\theta \rho_s})^2$, $p_2 = 1/(k_\theta^4 \rho_s^2 \hat{s}^4)\{\frac{1}{L_n^2} - [\frac{V_{\|o}}{C_s}(L_n^2/L_{v2}^2)\frac{1}{L_s \rho_s k_\theta}]^2/(\frac{L_n}{Rqk_\theta \rho_s})^2\}$, $x = k_\theta \rho \hat{s}$. Equation (3) is a simple Weber equation. When p_2 is positive and $\partial^2\Omega/\partial\chi_o^2 > 0$ ($\partial^2\Omega/\partial\chi_o^2 > 0$ is necessary in order that the mode be most unstable [10]), $A(x)$ is a localized Gaussian function. However, an important change is introduced by the velocity term. Assume $V_{\|oo} \sim C_s$ and, taking $L_s \sim qR$, we find that p_2 becomes negative if $L_n > L_{v2}$. $A(x)$ is then given by

$$A(x) = \exp\left[-i\frac{1}{2}\left(|p_2| \Big/ \left|\frac{\partial^2\Omega}{\partial\chi_0^2}\right|\right)^{1/2} x^2\right].$$

So, the mode envelope is now radially outgoing, which is reminiscent of the equivalent slab problem. Velocity curvature in the toroidal problem, similar to the magnetic shear in the corresponding slab problem, creates an *anti-well* in the radial direction (instead of the well formed by the diamagnetic frequency). The wave energy is therefore convected outward. The eigenvalue is given by

$$\Omega = \Omega_0 + \frac{p_1}{2} - i\frac{1}{2}\left(p_2 \left|\frac{\partial^2\Omega}{\partial\chi_0^2}\right|\right)^{1/2}.$$

The negative imaginary contribution in the eigenvalue shows that the velocity profile for negative value of the curvature *stabilizes* resistive drift-ballooning modes which otherwise escape magnetic shear damping. Coming to the experimental feasibility of obtaining the desired flow profile ($L_{v2} \sim L_{v1} \sim L_v \leq L_n$) envisioned in our model for stability, we have just started to measure the flow profile on the STOR-M with CT injection. The preliminary result indicates the existence of a toroidal flow during the transition. A detailed profile analysis is, however, yet to be done. The observation of toroidal flow of very high magnitude is, however, an expected result. This is because the previous measurements with the Mach probe during the positive biasing phase do indicate the existence of high toroidal flow velocities [8]. So, with the additional introduction of momentum by the tangential CT injection during the H-mode phase (which is automatically biased positively), toroidal velocity of even higher magnitude is most likely in the STOR-M. Since this high toroidal flow velocity has to disappear at the wall, a sharp gradient in the toroidal flow is expected in the edge of the STOR-M.

IV. Conclusions.—In summary, we have noted a novel feature of the H-mode induced by compact torus injection on the STOR-M tokamak. There is almost no change in the radial electric field profiles during and after the L-H transition. The usual hypothesis of the $\mathbf{E} \times \mathbf{B}$ shear stabilization mechanism is therefore unlikely to play a role in this transition. We suggest a new mechanism of the stabilization of microinstabilities by parallel flow as the plausible cause for the transition to this improved regime.

*Also at Hampton University, Hampton, Virginia 23668.

[1] C. Xiao, D. R. McColl, A. Hirose, and S. Sen, Fusion Energy 2000, Vienna, 2001 (IAEA, Paper No. EXP4/31).
[2] W. Zhang, C. Xiao, and A. Hirose, Phys. Fluids B **5**, 3961 1993).
[3] D. Biskamp and A. Zeiler, Phys. Rev. Lett. **74**, 706 (1995).
[4] J. F. Drake *et al.,* Phys. Rev. Lett. **77**, 494 (1996).
[5] S. Sen, Phys. Plasmas **2**, 2701 (1995); Phys. Lett. A **203**, 381 (1995).
[6] S. Sen, R. A. Cairns, R. G. Storer, and D. R. McCarthy, Phys. Plasmas **7**, 1192 (2000).
[7] L. Chen *et al.,* Nucl. Fusion **20**, 901 (1980).
[8] C. Xiao *et al.,* Phys. Plasmas **1**, 2291 (1994).
[9] S. Sen and A. Fukuyama, J. Fusion Energy **18**, 57 (1999).
[10] R. J. Hastie *et al.,* Nucl. Fusion **19**, 1223 (1979).